

Document downloaded from:

<http://hdl.handle.net/10251/154813>

This paper must be cited as:

Garro, E.; Barjau, C.; Gomez-Barquero, D.; Kim, J.; Park, S.; Hur, N. (2019). Layered Division Multiplexing with Distributed Multiple-Input Single-Output Schemes. IEEE Transactions on Broadcasting. 65(1):30-39. <https://doi.org/10.1109/TBC.2018.2823643>



The final publication is available at

<https://doi.org/10.1109/TBC.2018.2823643>

Copyright Institute of Electrical and Electronics Engineers

Additional Information

"© 2019 IEEE. Personal use of this material is permitted. Permission from IEEE must be obtained for all other uses, in any current or future media, including reprinting/republishing this material for advertising or promotional purposes, creating new collective works, for resale or redistribution to servers or lists, or reuse of any copyrighted component of this work in other works."

# Layered Division Multiplexing with Distributed Multiple-Input Single-Output Schemes

Eduardo Garro, Carlos Barjau, David Gomez-Barquero,  
Jeongchang Kim, Sung-Ik Park, and Namho Hur

**Abstract**—Single Frequency Networks (SFN) provides an increased spectral efficiency compared to the traditional Multiple Frequency Networks (MFN). However, some coverage areas in SFN can be affected by destructive interferences. In order to reduce these situations, distributed Multiple-Input Single-Output (MISO) schemes have been adopted in the new Digital Terrestrial Television (DTT) standards, Alamouti in DVB-T2 and Transmit Diversity Code Filter Sets (TDCFS) in ATSC 3.0. On the other hand, Layered Division Multiplexing (LDM), a Non-Orthogonal Multiple Access (NOMA) technology, has been adopted in ATSC 3.0 due to its spectral efficiency increase compared to Time or Frequency Division Multiplexing (TDM/FDM). The LDM signal is formed by a power superposition of two independent signals, which are designed for different reception conditions (mobile and fixed-rooftop). The combination of distributed MISO and LDM techniques has not been evaluated yet. In this paper the joint transmission of LDM with distributed MISO is analyzed in terms of complexity and the joint performance is evaluated by means of physical layer simulations.

**Index Terms**—Layered Division Multiplexing (LDM), Single Frequency Networks (SFN), Multiple-Input Single-Output (MISO), Alamouti, Transmit Diversity Code Filter Sets (TDCFS), ATSC 3.0, terrestrial broadcasting.

## I. INTRODUCTION

A Single Frequency Network (SFN) is constituted by several time and frequency synchronized transmitters, which send the same signal over the same Radio-Frequency (RF) channel. In comparison with the traditional Multiple Frequency Network (MFN), an SFN provides an increased spectral efficiency, as well as a homogeneous distribution of the received signal strength over the coverage area [1], [2]. Fig. 1 depicts an SFN with four transmitters as an example.

However, some SFN areas can suffer signal degradation. When the same signal from the different SFN transmitters arrive at receivers with similar magnitude and time of arrival but, with different phase, destructive interferences may occur. Therefore, severe multipath may come up [3], [4]. In order to limit these destructive interferences, distributed Multiple-Input

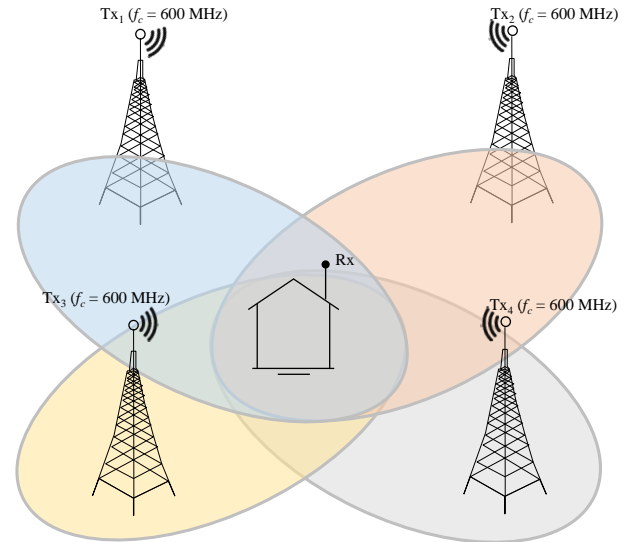


Fig. 1. Single Frequency Network (SFN) constituted by four transmitters that use the same RF frequency ( $f_c = 600$  MHz)

Single-Output (MISO) schemes have been adopted for the latest Digital Terrestrial Television (DTT) standards. Distributed algorithms alter the SFN, in such a way that the involved transmitters are still time and frequency synchronized, but the transmitted signal is modified. Two distributed MISO algorithms have been adopted in DTT standards, Frequency Pre-Distortion, such as Transmit Diversity Code Filter Sets (TDCFS) in ATSC 3.0 [5], and Space-Time/Frequency Block Coding (ST/FBC), such as Alamouti in DVB-T2 and DVB-NGH [6]. The benefits and constraints of them alone have been already analyzed. Nevertheless, the joint transmission of distributed MISO schemes with new transmission techniques is still missing.

Non-Orthogonal Multiple Access (NOMA), has emerged as a promising technique for New Radio 5G cellular systems [7]. In contrast to Orthogonal Multiple Access (OMA) solutions, such as Time or Frequency Division Multiplexing (TDM/FDM), each multiplexed service in NOMA utilizes 100% of frequency and time resources. Hence, NOMA can outperform OMA solutions [8]. ATSC 3.0 [9] has become as the first terrestrial broadcasting system that implements a NOMA solution, known as Layered Division Multiplexing (LDM) [10], [11]. The LDM signal consists of the superposition of two independent layers with different power levels. Each layer, defined as Core Layer (CL) and Enhanced Layer

This work was partially supported by the ICT R&D program of MSIP/IITP (No.2017-0-00081, Development of Transmission Technology for Ultra High Quality UHD), and by the Ministerio de Educación y Ciencia, Spain (TEC2014-56483-R), co-funded by European FEDER funds.

E. Garro, C. Barjau and D. Gomez-Barquero are with the Universitat Politècnica de Valencia, Valencia, 46022, Spain (e-mail: {edgarcre,carbarel,dagobar}@iteam.upv.es).

J. Kim is with the Division of Electronics and Electrical Information Engineering, Korea Maritime and Ocean University, Busan, Korea (e-mail: jchkim@kmou.ac.kr).

S.I. Park and N. Hur are with the Media Transmission Research Group, ETRI, Daejeon, Korea (e-mail: {psi76,namho}@etri.re.kr).

(EL) passes through a different Bit-Interleaved Coded Modulation (BICM) chain. Thus, each layer is designed with different robustness characteristics in order to target mobile reception conditions by the CL, and fixed-rooftop reception conditions by the EL.

Different studies for the joint transmission of LDM with other technologies, such as multi-RF channel (Channel Bonding) [12], [13], or Scalable High Efficiency Video Coding (SHVC) [14] have been already assessed. However, the joint transmission of distributed MISO schemes with LDM in an SFN has not been evaluated yet. This paper analyzes the implementation aspects at transmitter and receiver sides and it evaluates the joint performance of LDM with the two distributed MISO schemes (TDCFS and Alamouti). On the one hand, although the joint transmission of LDM and TDCFS is currently allowed by ATSC 3.0 standard, the joint performance was not evaluated during the standardization process. On the other had, the joint transmission of LDM with the well-known Alamouti scheme, adopted in DVB-T2 and DVB-NGH has not been assessed in the literature yet. The rest of the paper is structured as follows: Section II presents an overview of the distributed ATSC 3.0 TDCFS, and DVB-T2 Alamouti schemes. Next, the potential transmitter and receiver implementation aspects of the joint transmission with LDM are analyzed in Section III. Section IV describes the simulation setup followed for the performance evaluation, which is presented in Section V. Last, conclusions are drawn in Section VI.

## II. MISO BACKGROUND

### A. Frequency pre-distortion

The frequency pre-distortion approach de-correlates the signals from the different transmitters using a specific linear phase-distortion algorithm. This pre-distortion has to be unique for each transmitter and has to be different across OFDM subcarriers. This de-correlation enhances the frequency selectivity at receivers so that destructive cancellations are prevented. There are two techniques: the so-called enhanced SFN (eSFN), which was adopted in DVB-NGH [6], and TDCFS, adopted in ATSC 3.0. Compared to eSFN, TDCFS provides a higher decorrelation of the signal in the frequency domain and, thus, an overall better performance [5].

1) *TDCFS in ATSC 3.0*: The linear frequency domain filters are all-pass filters with minimized cross-correlation under the constraints of the number of transmitters  $M \in \{2, 3, 4\}$  and the time domain span of the filters  $L \in \{64, 256\}$ . Code filter frequency domain pre-distortion function  $C_x[i]$  is determined using the time domain impulse response vectors  $h_x[n]$  and using a zero-padded Fast Fourier Transform (FFT) of size  $N_{FFT}^m$  associated with current subframe  $m$ . They are introduced in such a way that special signal processing at the receivers is not necessary, since  $C_x[i]$  are seen by the receivers as a part of the channel. Thus, baseline receivers can also exploit the diversity introduced by these MISO schemes. They are calculated as:

$$C_x[i] = \exp \left[ j \arg \left( \sum_{n=0}^{L-1} h_x[n] e^{-\frac{j2\pi in}{N_{FFT}^m}} \right) \right] \quad (1)$$

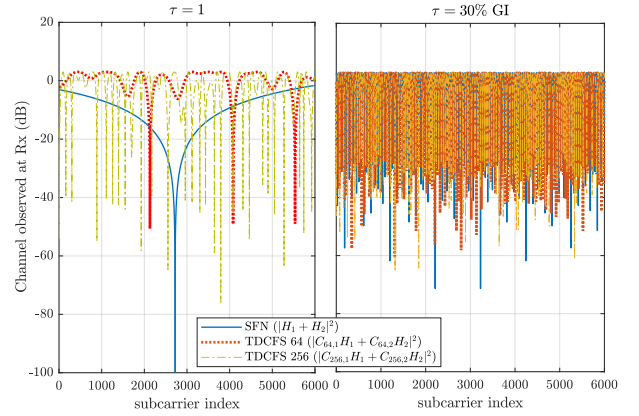


Fig. 2. Channel frequency response of an SFN with two transmitters and when TDCFS is applied ( $L = 64$ , and  $L = 256$ ) (delays  $\tau = 1$ , and 30%GI samples)

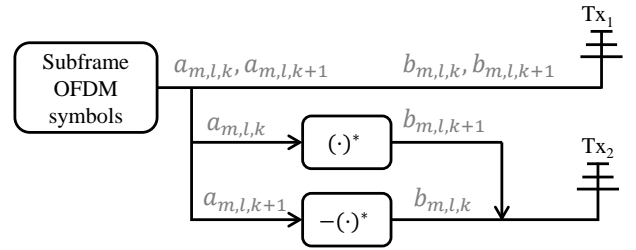


Fig. 3. MISO Alamouti encoder processing on DTT systems

where  $n$  stands for filter index  $n \in \{0, \dots, L-1\}$ ,  $h_x[n]$  are provided in [15], and  $x$  is the transmitter index  $x \in \{1, \dots, M\}$ . Subcarrier index  $i \in \{0, \dots, NoC-1\}$ , where  $NoC$  is the number of active carriers associated to the current subframe.

Fig. 2 shows the channel frequency response (CFR) of an SFN with two transmitters and different delays when TDCFS is applied and when it is not (SFN). As it can be observed, TDCFS pre-distortion modifies the CFR so that no deep fading occurs even at short echo delays. It can also be observed that for medium echo delays (in this case 30% of Guard Interval (GI) samples) no performance differences are expected between SFN and TDCFS since the CFRs seem to be equivalent.

### B. Space-Time/Frequency Block Coding (ST/FBC)

In the case of ST/FBC, the data stream to be transmitted is encoded in pair of orthogonal blocks, which are distributed among spaced antennas and across time/frequency. Alamouti encoding is the simplest orthogonal design of all the complex-valued ST/FBCs, but at the same time is the only ST/FBC achieving rate-1 [16].

1) *Alamouti in DVB-T2/DVB-NGH*: An Alamouti encoding variant has been adopted in DVB-T2 and DVB-NGH. In particular, the pair of time indices is replaced by a pair of frequency indices to form an orthogonal Space Frequency Block Code (SFBC). The Alamouti encoding divides the available transmit antennas into two groups. The pair of cells  $\{a_{m,l,k}, a_{m,l,k+1}\}$  from group 1 are not modified. On the

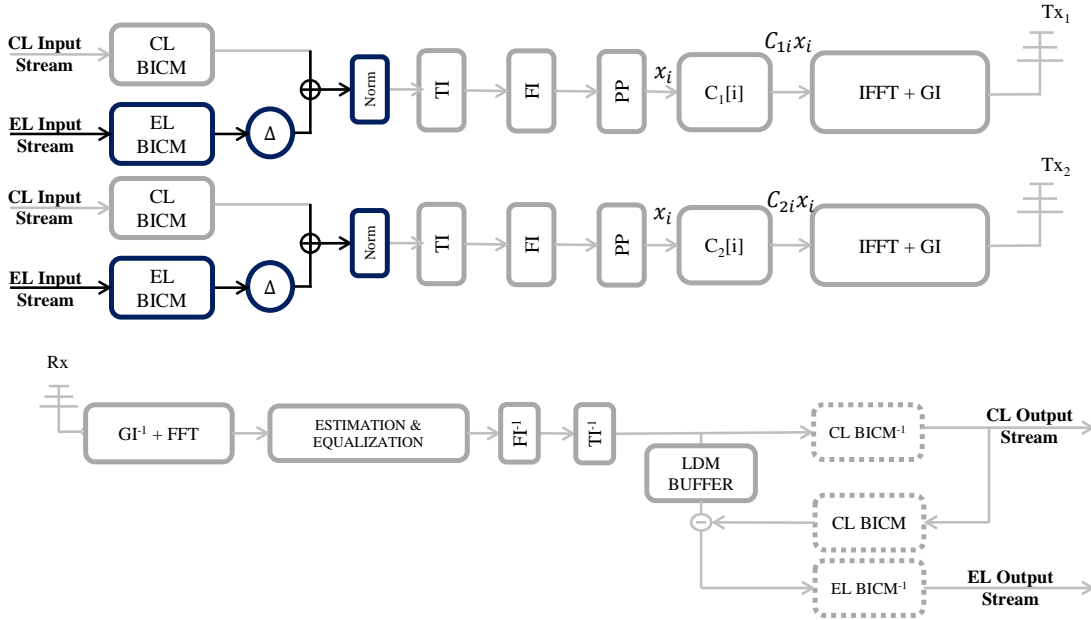


Fig. 4. Joint MISO TDCFS and LDM block diagram with two transmitters (top) and receiver (bottom)

other hand,  $\{a_{m,l,k}, a_{m,l,k+1}\}$  are complex-conjugated and interleaved from transmit antennas of group 2. The output cells  $\{b_{m,l,k}(\text{Tx}_1), b_{m,l,k}(\text{Tx}_2)\}$  for group 1 and 2, respectively are thus encoded according to:

$$\begin{aligned} b_{m,l,k}(\text{Tx}_1) &= a_{m,l,k}, & b_{m,l,k+1}(\text{Tx}_1) &= a_{m,l,k+1} \\ b_{m,l,k}(\text{Tx}_2) &= -a_{m,l,k+1}^*, & b_{m,l,k+1}(\text{Tx}_2) &= a_{m,l,k}^* \end{aligned} \quad (2)$$

where  $l$  denotes the OFDM symbol index,  $m$  denotes the frame index,  $k$  denotes the data carrier index ( $k = \{0, 2, 4, 6, \dots, N_{data}\}$ ), and  $N_{data}$  is the number of data carriers in an OFDM symbol. The encoding process is illustrated in Fig. 3.

Alamouti encoding requires not only additional complexity at the transmitter but also at the receiver. Although only a single receiving antenna is needed, the estimation of the CFRs of both transmitted MISO groups is required. Thus, orthogonal pilot patterns should be used between groups. This means that the number of pilots must be doubled for the same channel estimation resolution, so that this pilot overhead should be considered when evaluating the Alamouti gains in terms of spectral efficiency [17]. In addition, MISO Alamouti requires of an additional equalization process for recovering the components from the combined signals.

### III. IMPLEMENTATION ASPECTS OF LDM WITH MISO SCHEMES ON ATSC 3.0

This section evaluates the implementation aspects for ATSC 3.0 transmitters and receivers due to the joint LDM and MISO scheme transmission. Although ATSC 3.0 has only adopted TDCFS as a distributed MISO scheme, Alamouti is also considered in order to provide a more complete study.

#### A. LDM with MISO TDCFS

Fig. 4 illustrates the joint transmission of LDM and MISO TDCFS (top) and a LDM baseline receiver (bottom) block

diagrams, when the network is constituted by two transmitters. The two transmitters followed the same block diagram except for the different TDCFS pre-distortion function. Hence, one BICM chain per LDM layer is applied on each transmitter (CL BICM and EL BICM). The layers are then aggregated with same power allocation controlled by an Injection Level ( $\Delta$ ) on the two transmitters. Time Interleaver (TI) and Frequency Interleaver (FI) are also equally implemented on both transmitters. Therefore, the same  $x_i = CL_i + EL_i$  LDM signal can be observed at this point on both transmitters. Next, a different TDCFS pre-distortion function  $C_x[i]$  is applied per transmitter, so that whereas Tx<sub>1</sub> transmits  $C_{1i}x_i$ ,  $C_{2i}x_i$  is transmitted from Tx<sub>2</sub>. Finally, inverse-FFT is applied and GI is inserted. From the figure, when LDM is jointly used with MISO TDCFS no extra constraints are found, further than those related to each technology by itself. In addition, since TDCFS pre-distortion filters are applied to the combined LDM signal, same MISO gains in both layers are expected.

At the receiver, after removing GI and applying the FFT, the complex-valued received signal is modelled as:

$$y_i = (h_{1,i} \cdot C_1[i] + h_{2,i} \cdot C_2[i]) \cdot x_i + n_i \quad (3)$$

where  $(h_{1,i} \cdot C_1[i] + h_{2,i} \cdot C_2[i])$  is assumed by receiver's channel estimator as the CFR and  $n_i$  is the AWGN noise. Next, de-interleaving processes are performed. Then, CL is first demodulated, and cancelled for the EL demodulation.

#### B. LDM with MISO Alamouti

In the same way it was shown in previous section, Fig. 5 illustrates the joint transmission of LDM with MISO Alamouti (top) and an LDM with MISO Alamouti decoding receiver (bottom) block diagrams, when the network is constituted by two transmitters.

Similar process as with TDCFS is done until MISO Alamouti encoding is performed in each transmitter. Next, whereas



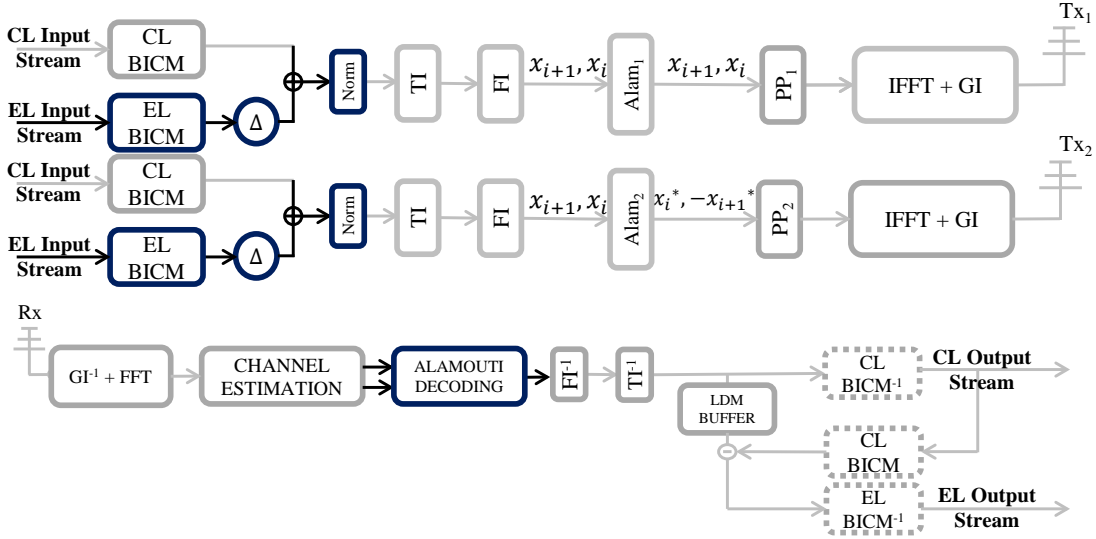


Fig. 5. Joint MISO Alamouti and LDM block diagram with two transmitters (top) and receiver (bottom)

none processing is applied to  $x_i$  LDM signal in Tx<sub>1</sub>, Alamouti encoding processes complex conjugate and pairwise interleave  $x_i$  in Tx<sub>2</sub>. After Alamouti encoding is processed, orthogonal pilot patterns are applied to each transmitter. Finally, IFFT and GI are applied and inserted similarly to the two transmitters. As the same  $x_i = CL_i + EL_i$  LDM signal is employed at Alamouti encoding process, it could be considered that the main MISO Alamouti benefits can also be achieved by both layers.

At the receiver, after removing GI and applying the FFT, the complex-valued received signal is modelled as:

$$\begin{aligned} y_i &= h_{1,i} \cdot (x_i) - h_{2,i} \cdot (x_{i+1})^* + n_i \\ y_{i+1} &= h_{1,i+1} \cdot (x_{i+1}) + h_{2,i+1} \cdot (x_i)^* + n_{i+1} \end{aligned} \quad (4)$$

The received signals  $y_i$  and  $y_{i+1}$  are a combination of the two pair of transmitted cells  $x_i$  and  $x_{i+1}$ . Therefore, in order to extract  $x_i$  and  $x_{i+1}$ , an Alamouti decoding process is needed after the two CFRs ( $h_1$  and  $h_2$ ) have been obtained by the channel estimator. This equalization process is performed as:

$$\begin{bmatrix} y_i \\ y_{i+1}^* \end{bmatrix} = \begin{bmatrix} h_{1,i} & -h_{2,i} \\ h_{2,i+1}^* & h_{1,i+1} \end{bmatrix} \begin{bmatrix} x_i \\ x_{i+1}^* \end{bmatrix} + \begin{bmatrix} n_i \\ n_{i+1}^* \end{bmatrix} \quad (5)$$

After Alamouti decoding, de-interleaving processes are performed before CL demodulation. If the receiver is expected to retrieve EL, before its demodulation, CL is remodulated and cancelled. As it can be observed, MISO Alamouti requires of a more complex channel estimation process (two channel estimates are needed) and an extra decoding at receivers. These blocks are not very complex, but it is evident that the complexity is increased with respect to the previous configuration.

#### IV. METHODOLOGY AND SIMULATION SETUP

##### A. Methodology

The performance of LDM and MISO schemes is evaluated by means of physical layer simulations with a software simulator validated during the ATSC 3.0 standardization process.

TABLE I  
BICM AND WAVEFORM PARAMETERS

BICM	Waveform	
Core Layer QPSK 4/15	CTI = 1024 rows	BW = 6 MHz
Enhanced Layer 64NUC 10/15	Pilot $D_x = 6$	Pilot boosting = 4
$\Delta = \{2 - 6\}$ dB	FFT = 16k	GI = 1024 samples

The performance of the MISO schemes on both layers is compared with the transmission when no pre-processing is applied to the transmitted signal (SFN). In order to provide a fair comparison among the three configurations (SFN, MISO TDCFS and MISO Alamouti), different scenarios have been assumed with realistic channel estimation.

##### B. Transmission Setup

The common transmitted parameters are introduced in Table I.

1) *Pilot considerations*: On the one hand, a SISO pilot pattern will be used on TDCFS performance evaluation. On the other hand, a MIMO pilot pattern must be used with MISO Alamouti scheme. In [18] it was shown that for the FFT 16k - GI 1024 samples, and when a frequency FFT interpolator is used at receivers,  $D_x = 6$ ,  $D_y = 2$  pilot pattern with the maximum pilot boosting power provided the best performance (around 1 dB gain compared to no boosting). Therefore, ATSC 3.0 *SP6\_2* with ATSC 3.0 pilot boosting 4 is assumed for the performance simulations in TDCFS. This means that the pilot carriers are power boosted 4.6 dB with respect to data carriers' power. Regarding Alamouti pilot configuration, it should be noticed that ATSC 3.0 MIMO pilots fall on exactly the same positions as for SISO. Thus, *MP6\_2* with pilot boosting 4 is used in Alamouti results.

Nevertheless, the amplitudes and/or phases of MIMO pilots may be modified depending on the MIMO pilot antenna

TABLE II  
MP  $D_x$  AND  $D_y$

SISO	MIMO	
	WH encoding	NP encoding
$D_x$	$2D_x$	$D_x$
$D_y$	$D_y$	$2D_y$

TABLE III  
SFN SCENARIOS UNDER STUDY

Scenario	Transmitters	$\tau$ (% GI)
1	2	0, 0
2	2	0, 1.3
3	2	0, 90
4	3	0, 18, 90
5	4	0, 18, 70, 90
6	5	0, 18, 23, 70, 90
7	8	0, 1.3, 18, 23, 50, 70, 90, 95

encoding, Walsh-Hadamard (WH) or Null Pilot (NP). In WH, whereas pilots from  $Tx_1$  are not modified, pilots from  $Tx_2$  are partitioned into two subsets. Phases of the pilots of first subset are not modified, but phases of pilots of second subset are inverted. Thus, the Doppler limit of WH channel estimation is the same as SISO, but the Nyquist limit is halved. On the other hand, in NP encoding, the amplitudes of the scattered pilots of both subsets are modified in both signals transmitted from  $Tx_1$  and  $Tx_2$ .  $Tx_1$  alternately transmits scattered pilots with 3 dB increased transmit power and scattered pilots with null power (zero amplitude). Scattered pilots of  $Tx_2$  are transmitted with null power and with 3 dB gain in reverse order. As a result, for NP, the Doppler limit of channel estimation falls to half compared to SISO, but the Nyquist limit keeps the same. As summary, the equivalent values of  $D_x$  and  $D_y$  of each MIMO pilot encoding are summarized in Table II. Both pilot encodings are analyzed for Alamouti in Section V-B.

2) *TDCFS considerations*: Filter length  $L = 256$  samples is assumed on SFN scenarios with four or less transmitters, as it provides a better performance than  $L = 64$  samples [5]. A combination of both filter lengths was assumed on scenarios with SFNs constituted by five and eight transmitters.

### C. SFN scenarios

The SFN scenarios under evaluation can be grouped in two studies. A first study with just two transmitters but with different delays (0 samples, 1.3% of GI samples, and 90% of GI samples) is assumed. Next, scenarios with more than two transmitters are evaluated. The time of arrival of each transmitter in every scenario is summarized in Table III. Regarding echo amplitudes, in order to provide the most challenging SFN conditions, it has been assumed that all echoes arrive at receiver with same magnitude, i.e. 0 dB echo is always assumed. Fig. 6 illustrates the Power Delay Profile (PDP) for scenario 7.

When more than two transmitters are considered, different alternatives can be assumed for MISO Alamouti grouping, as

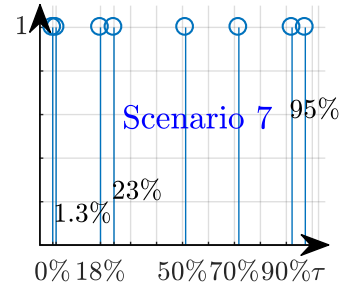


Fig. 6. Power Delay Profile of scenario 7. The rest of scenarios are constituted by a subset of this one.

TABLE IV  
GROUPING ALTERNATIVES FOR SCENARIOS 4 AND 5

Grouping	Scenario 4 (3 Tx)		Scenario 5 (4 Tx)	
	Group 1	Group 2	Group 1	Group 2
1	0-90	18	0-70	18-90
2	0-18	90	0-18	70-90
3	18-90	0	0-90	18-70

well as for MISO TDCFS filtering. Table IV presents the potential grouping alternatives for scenarios 4, and 5, and Table V for scenario 6. Due to the big amount of grouping alternatives for the performance evaluation of scenario 7, only 0-18-50-90 and 1.3-23-70-95 for group 1 and group 2, respectively, alternative has been evaluated.

For obtaining the CL performance in mobility conditions, a TU-6 realization with a Doppler shift  $f_D = 33.3$  Hz is applied to each transmitter path. Regarding EL performance evaluation, uncorrelated realizations with same magnitude but different random phase are applied in order to observe the most destructive interference fixed reception conditions.

### D. Receiver configuration

A Least-Square (LS) estimation with a moving average time interpolation and a FFT frequency interpolation are considered for the channel estimator. In addition, an MMSE equalizer is assumed. During the process, it was observed that the performance of the channel estimator mainly depends on the filtering window length of the FFT frequency interpolator. On the one hand, the window length should be sufficiently long for tracing the different echoes of the SFN scenarios. On the other hand, the window length should be as short as possible but without ruling out any echo in order not to increase the frequency domain noise bandwidth.

In order to provide a fair comparison for the whole SFN profiles defined in previous section, three different window lengths were evaluated:

- 1) 95% of GI window length for post-echoes and 10% for pre-echoes.
- 2) 95% of GI window length + 256 samples of TDCFS filtering for post-echoes and 10% for pre-echoes.
- 3) 95% of FFT/ $D_x$  window length for post-echoes and 10% for pre-echoes.

TABLE V  
GROUPING ALTERNATIVES FOR SCENARIO 6 (5 TRANSMITTERS)

Grouping	Group 1	Group 2	Grouping	Group 1	Group 2
1	0-23-90	18-70	6	0-18-90	23-70
2	0-18-23	70-90	7	18-23-70	0-90
3	0-18-70	23-90	8	18-23-90	0-70
4	0-23-70	18-90	9	18-70-90	0-23
5	0-70-90	18-23	10	23-70-90	0-18

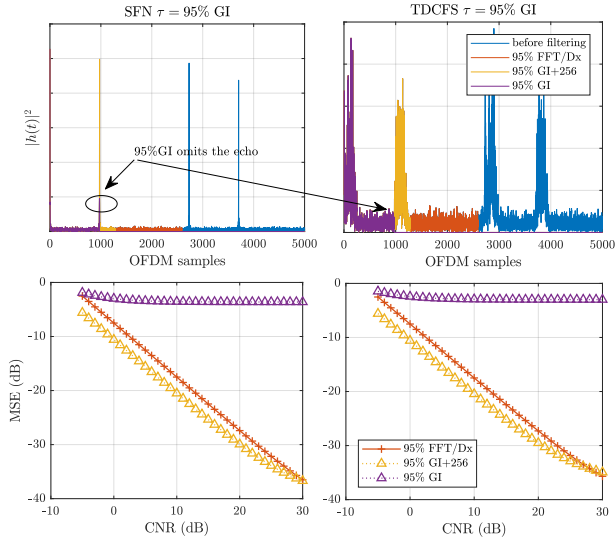


Fig. 7. Top: SFN (left) and TDCFS (right) channel impulse response in a 0 dB echo channel with  $\tau = 95\%$  GI delay. Bottom: MSE of channel estimator with different FFT frequency interpolators for SFN (left) and TDCFS (right).

For the transmitting configuration under study the window lengths in number of samples are:

- 1)  $\lceil 95\% \cdot 1024 \rceil = 973$ , and  $\lceil 10\% \cdot 1024 \rceil = 103$ .
- 2)  $\lceil 95\% \cdot 1024 + 256 \rceil = 1229$ , and  $\lceil 10\% \cdot 1024 \rceil = 103$ .
- 3)  $\lceil 95\% \cdot \frac{16 \cdot 1024}{6} \rceil = 2595$ , and  $\lceil 10\% \cdot \frac{16 \cdot 1024}{6} \rceil = 274$ .

The performance of the different window lengths was evaluated by comparing the Minimum Square Error (MSE) of the channel estimator for the 95% of GI echo delay. Top part of the Fig. 7 depicts the channel impulse responses filtered on this scenario with the three configurations and when TDCFS pre-distortion is disabled (left) and enabled (right). Bottom part of Fig. 7 provides the MSE for the different configurations under consideration.

From top part of the figure it can be seen that the echo is not fully covered by the shortest window length (95% GI length - purple graph) when TDCFS is applied and when it is not. The omission of the echo is translated in a bad channel estimation, as it is observed in the bottom part. Therefore, this window length is discarded for the performance evaluation of all the proposed SFN profiles. When the other two configurations are compared, it can be observed that 95% of GI window length + 256 samples provides a lower MSE. Hence, taking into account all the potential echo delays, the GI + TDCFS samples length is considered as a valid window filtering length, and it is adopted for the rest of the studies.

TABLE VI  
CL CNR THRESHOLD (DB) AT BER =  $10^{-4}$  FOR ALL THE SCENARIOS UNDER EVALUATION

Scenario	MISO Alamouti (NP)	MISO TDCFS	SFN
1	4.0	4.2	5.1
2	4.0	4.2	4.1
3	3.9	4.1	4.1
4	3.6	3.8	3.8
5	3.1	3.4	3.4
6	2.9	3.2	3.3
7	2.7	3	3

## V. LDM AND DISTRIBUTED MISO PERFORMANCE EVALUATION

This section studies the potential gains offered by the joint configuration of MISO TDCFS or MISO Alamouti with LDM in comparison with the use of none MISO technique on SFN scenarios. It is divided in three subsections. Subection V-A evaluates and compares the performance of the CL for all the defined scenarios in previous section. Next, subsection V-B compares the EL performance for all the scenarios with the three schemes in the same manner as in the CL studies. The performance of both LDM layers is analyzed for an injection level  $\Delta = 4$  dB. The third subsection analyzes the influence of  $\Delta$  on MISO Alamouti and MISO TDCFS gains for both LDM layers.

### A. Core Layer Performance

1) *Scenarios 1, 2, and 3 (2 transmitters)*: Left part of Fig. 8 depicts the CL performance for the three scenarios with two transmitters. In general, it can be observed that the performance among the three schemes is very similar regardless of the echo delay. Only at  $\tau = 0\%$  echo delay, 0.8 dB gains can be observed when MISO Alamouti (with NP encoding) or MISO TDCFS is enabled. As the TU-6 paths form a non-static channel, TI can obtain enough diversity. Thus, additional MISO spatial diversity gain is not significant. This is known as the *diminishing marginal returns of diversity* [19].

2) *Scenarios 4, 5, 6, and 7 (more than 2 transmitters)*: Right part of Fig. 8 depicts the CL performance for the different grouping alternatives of the scenarios with more than two transmitters. It can be firstly observed that MISO Alamouti (with NP encoding) slightly outperforms SFN and MISO TDCFS by 0.3 dB in all scenarios. It can also be observed that the performance of the three schemes is not modified whether one grouping alternative is assumed. One last conclusion that can be extracted from Fig. 8 is that the overall performance of the three schemes increases with the number of transmitters because of the additional diversity.

The CNR thresholds for the three schemes and seven scenarios are summarized in Table VI. In summary, it can be concluded that for mobile environments, where the CL is traditionally planned, small gains are obtained by distributed MISO schemes, so that they do not provide a significant performance increase.

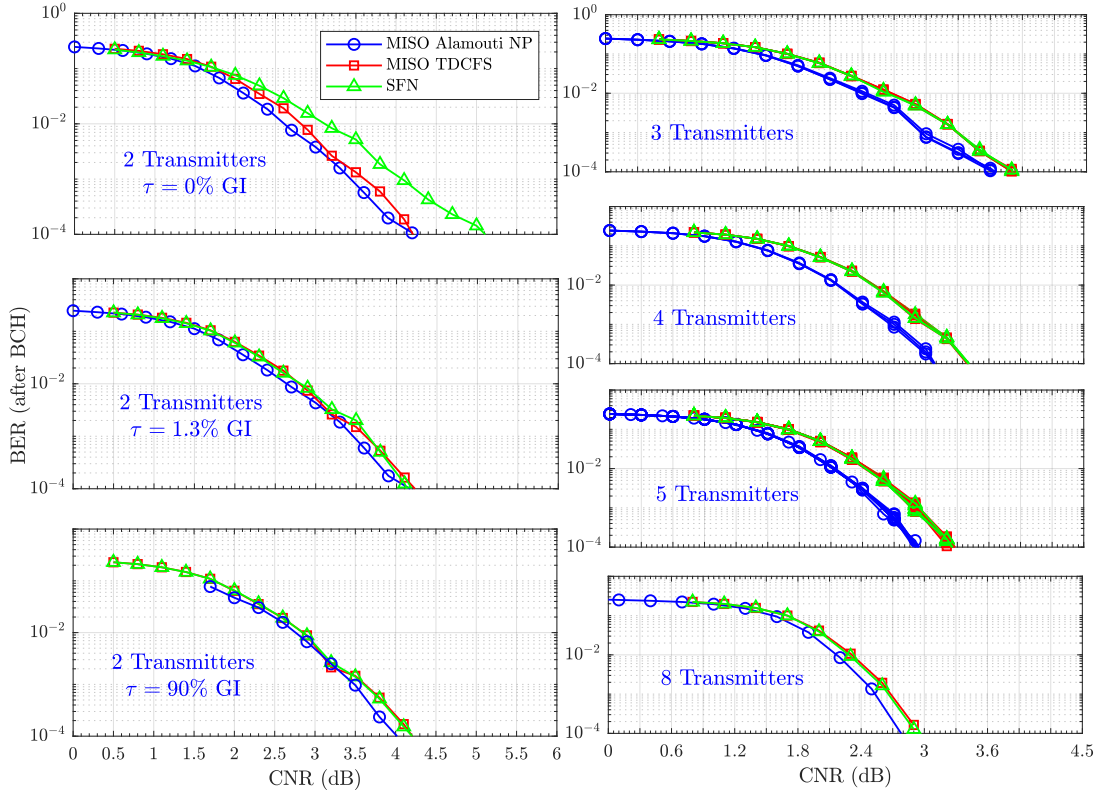


Fig. 8. Core Layer performance with SFN, MISO TDCFS and MISO Alamouti schemes (with NP encoding) for all the SFN scenarios under study. LDM injection level  $\Delta = 4$  dB. Left: scenarios with two transmitters, delayed by  $\tau = 0\%$  (top),  $\tau = 1.3\%$  (middle), and  $\tau = 90\%$  (bottom) GI samples. Right: scenarios with three, four, five and eight transmitters. Uncorrelated TU-6 channel realizations with Doppler shift  $f_D = 33.3$  Hz are applied to each path.

### B. Enhanced Layer Performance

For this layer, the two ATSC 3.0 MIMO pilot encodings have been considered on MISO Alamouti scheme.

1) *Scenarios 1, 2, and 3 (2 transmitters)*: Left part of Fig. 9 illustrates the EL performance for the SFN scenarios constituted by two transmitters with the three schemes. It can be seen that for fixed reception conditions, Alamouti with NP encoding now increases the performance up to 3 dB with respect to SFN. It is explained because TI is not providing any time diversity, and because of the higher spatial diversity at high SNR regions. It can also be noticed that SFN cannot achieve Quasi-Error Free (QEF) conditions for the null echo delay. Nevertheless, this SFN scenario is improved when MISO TDCFS is applied. On the other hand, at short echo delays (such as 1.3% of GI samples), TDCFS provides a worse performance (-0.3 dB) than SFN because of its additional frequency selectivity. If both MIMO pilot encodings are compared, it can be observed that, as it was expected, NP is always outperforming WH. This better performance comes from the 3 dB boosting at low echo delay SFN profiles, and from the higher echo tolerance at high echo delays.

2) *Scenarios 4, 5, 6, and 7 (more than 2 transmitters)*: The EL performance for the different grouping alternatives of scenarios 4-7 is presented in right part of Fig. 9. It can be seen that, similarly than previous scenarios, MISO Alamouti NP outperforms the other schemes. Nevertheless, these gains are reduced to approximately 1.7 dB. The reason comes from the

TABLE VII  
EL CNR THRESHOLD (DB) AT BER =  $10^{-4}$  FOR ALL THE SCENARIOS UNDER EVALUATION

Scenario	MISO Alamouti (NP)	MISO TDCFS	SFN
1	18.8	22.4	NA
2	18.8	22.4	21.7
3	19.0	21.7	21.7
4	19.4	21.1	21.1
5	19.7	21.5	21.4
6	19.7	21.6	21.5
7	20.1	21.8	21.7

non-optimal Alamouti configuration of only two transmitters involved in the SFN. Again, NP is also outperforming WH. One last conclusion that can be derived from the figure is that the overall performance decreases with the number of transmitters because of the frequency selectivity increase.

The EL CNR thresholds in dB for the three schemes and seven scenarios are summarized in Table VII. In summary, it can be concluded that for fixed environments, where the EL is usually assigned for, MISO Alamouti provides from 1.7 dB to 3 dB gains. Hence, the inclusion of this MISO scheme in the ATSC 3.0 standard is recommended.



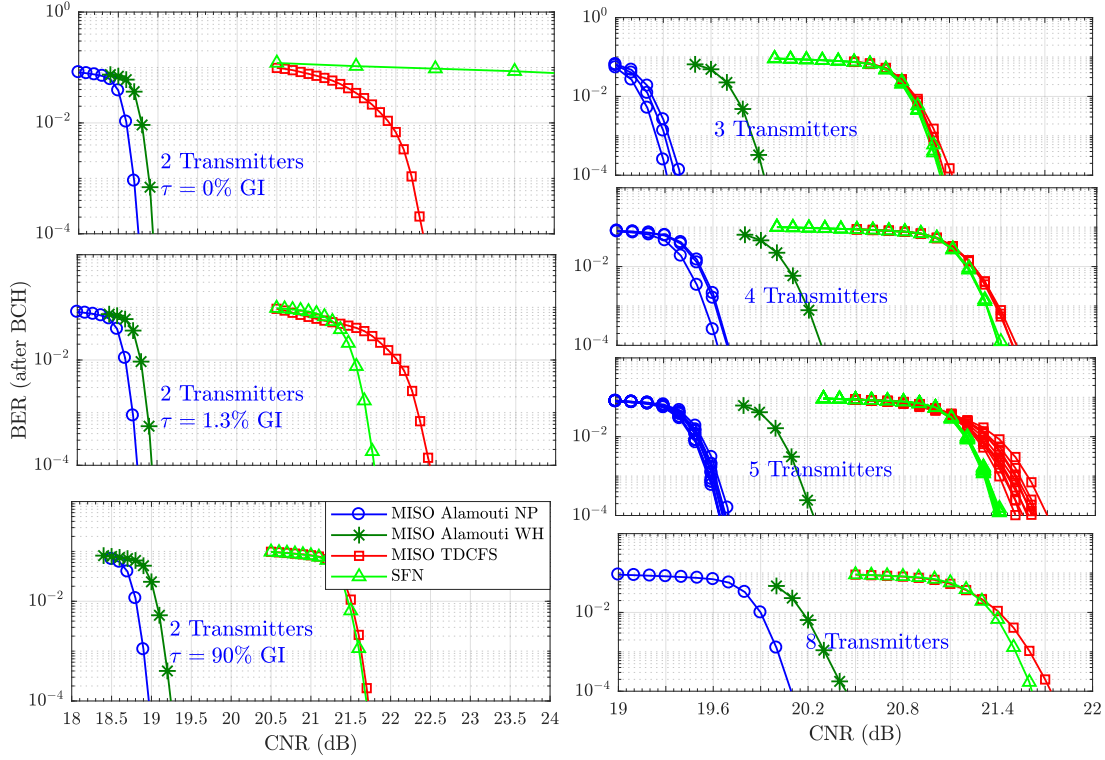


Fig. 9. Enhanced Layer performance with SFN, MISO TDCFS and MISO Alamouti schemes for all the SFN scenarios under study. LDM injection level  $\Delta = 4$  dB. Left: scenarios with two transmitters, delayed by  $\tau = 0\%$  (top),  $\tau = 1.3\%$  (middle), and  $\tau = 90\%$  (bottom) GI samples. Right: scenarios with three, four, five and eight transmitters. Uncorrelated realizations with same magnitude but different random phase are applied to each channel path. Both MIMO pilot encodings have been considered (Null Pilots - NP, Walsh-Hadamard - WH).

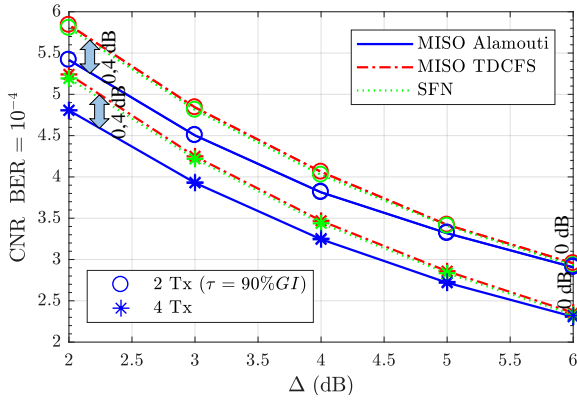


Fig. 10. Core Layer performance with SFN, MISO TDCFS and MISO Alamouti schemes for  $\Delta = \{2-6\}$  dB. MIMO NP encoding is assumed for MISO Alamouti.

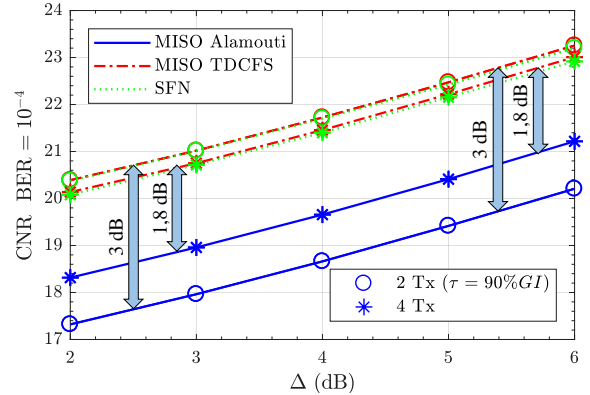


Fig. 11. Enhanced Layer performance with SFN, MISO TDCFS and MISO Alamouti schemes for  $\Delta = \{2-6\}$  dB. MIMO NP encoding is assumed for MISO Alamouti.

### C. Influence of Injection Level ( $\Delta$ )

Previous sections evaluated the performance for the different MISO schemes with a fixed  $\Delta = 4$  dB value. This section aims at evaluating the influence of  $\Delta$  in a wider range. Concretely,  $\Delta = \{2-6\}$  dB is considered. Scenarios 3 (2 transmitters,  $\tau = 90\%$ GI) and 5 (4 transmitters) are only considered, since they can be assumed as the two most representative SFN scenarios. Fig. 10 illustrates the CL performance, whereas Fig. 11 depicts the Enhanced Layer performance.

From Fig. 10, it can be observed that the performance of the

three schemes is alike, because of the previously time diversity added by TI. Nevertheless, small Alamouti gains can be obtained at lower  $\Delta$  values, because of the inherent behaviour of Alamouti, where gains increase with CNR region. Finally, it can also be seen that the performance increase thanks to the additional time diversity of 4 transmitters scenario remains at 0.6 dB regardless of  $\Delta$ . Regarding EL performance, from Fig. 11, the same conclusions extracted from Section V-B to  $\Delta = 4$  dB can be applied to other values: on the one hand, Alamouti always outperforms the other two configurations.

Maximum gains of 3 dB are achieved on two transmitters scenario, whereas these gains are reduced to 1.7 dB on four transmitters scenario. Therefore, Alamouti scheme is considered as an optimum configuration for both LDM layers, and in particular for the EL, where up to 3 dB performance gains can be achieved compared to MISO TDCFS and SFN schemes.

## VI. CONCLUSIONS

This paper studies the joint transmission of ATSC 3.0 Layered Division Multiplexing (LDM) mode with distributed Multiple-Input Single-Output (MISO) schemes. Two alternatives have been considered, ATSC 3.0 predistortion scheme, namely TDCFS, and DVB-T2 Space Frequency Block Code scheme, also known as MISO Alamouti. Whereas TDCFS de-correlates the signals from the different transmitters to avoid destructive interferences, Alamouti encoding achieves full diversity by sending the same but orthogonal signals between transmitters. This is done in pair of consecutive cells. On the one hand, although the joint transmission of LDM and TDCFS is currently allowed by ATSC 3.0, the joint performance was not evaluated during the standardization process. On the other hand, the joint transmission of LDM with the MISO Alamouti scheme is also analyzed in order to provide a comparison between the different distributed MISO schemes in the literature.

Regarding the implementation aspects, it was observed that the LDM layers are aggregated before any waveform processing, like MISO schemes. Hence, the combination of LDM with the two distributed MISO schemes under consideration, TDCFS and Alamouti, does not require extra complexity constraints, further than those related to each technology by itself.

For the simulated performance evaluation, seven SFN scenarios with different echo delays ( $\tau$ ) and number of transmitters were considered. No significant MISO gains were obtained for the CL. The MISO spatial diversity gain is not significant because of the time diversity provided by the prior Time Interleaver (TI). Regarding the performance of the Enhanced Layer (EL), on the one hand Alamouti gains from 3 dB to 1.8 dB were achieved for scenarios with two transmitters and more, respectively. These gains are achieved with the MIMO Null Pilot encoding (MIMO NP), which outperforms the traditionally Walsh-Hadamard encoding used in DVB systems. On the other hand, TDCFS gains were only shown at the most challenging scenario, where one echo arrives at the same time and magnitude but with inverse phase.

Overall, since Alamouti gains of up to 3 dB can be achieved, it is proposed to be included into the next DTT standard, despite it requires of a more complex receiver.

## REFERENCES

- [1] A. Mattsson, "Single Frequency Networks in DTV," *IEEE Trans. Broadcast.*, vol. 51, no. 4, pp. 413–422, Dec 2005.
- [2] D. Plets *et al.*, "On the Methodology for Calculating SFN Gain in Digital Broadcast Systems," *IEEE Trans. Broadcast.*, vol. 56, no. 3, pp. 331–339, Sept 2010.
- [3] G. Santella, R. D. Martino, and M. Ricchiuti, "Single Frequency Network (SFN) Planning for Digital Terrestrial Television and Radio Broadcast Services: the Italian Frequency Plan for T-DAB," in *2004 IEEE 59th Vehicular Technology Conference (VTC)*, vol. 4, May 2004, pp. 2307–2311.
- [4] J. Morgade *et al.*, "SFN-SISO and SFN-MISO Gain Performance Analysis for DVB-T2 Network Planning," *IEEE Trans. Broadcast.*, vol. 60, no. 2, pp. 272–286, June 2014.
- [5] S. LoPresto, R. Citta, D. Vargas, and D. Gomez-Barquero, "Transmit Diversity Code Filter Sets (TDCFSs), an MISO Antenna Frequency Predistortion Scheme for ATSC 3.0," *IEEE Trans. Broadcast.*, vol. 62, no. 1, pp. 271–280, March 2016.
- [6] J. Robert and J. Zollner, "Multiple-Input Single-Output Antenna Schemes for DVB-NGH," in *Next Generation Mobile Broadcasting*, D. Gomez-Barquero, Ed. Boca Raton, FL, USA: CRC Press, 2013, pp. 581–608.
- [7] L. Dai *et al.*, "Non-Orthogonal Multiple Access for 5G: Solutions, Challenges, Opportunities, and Future Research Trends," *IEEE Communications Magazine*, vol. 53, no. 9, pp. 74–81, September 2015.
- [8] D. Gomez-Barquero and O. Simeone, "LDM Versus FDM/TDM for Unequal Error Protection in Terrestrial Broadcasting Systems: An Information-Theoretic View," *IEEE Trans. Broadcast.*, vol. 61, no. 4, December 2015.
- [9] L. Fay, L. Michael, D. Gomez-Barquero, N. Ammar, and M. W. Caldwell, "An Overview of the ATSC 3.0 Physical Layer Specification," *IEEE Trans. Broadcast.*, vol. 62, no. 1, March 2016.
- [10] L. Zhang *et al.*, "Layered Division Multiplexing: Theory and Practice," *IEEE Trans. Broadcast.*, vol. 62, no. 1, March 2016.
- [11] S. I. Park *et al.*, "Low Complexity Layered Division Multiplexing System for ATSC 3.0," *IEEE Trans. Broadcast.*, vol. 62, no. 1, March 2016.
- [12] E. Garro, J. J. Gimenez, S. I. Park, and D. Gomez-Barquero, "Layered Division Multiplexing With Multi-Radio-Frequency Channel Technologies," *IEEE Trans. Broadcast.*, vol. 62, no. 2, pp. 365–374, June 2016.
- [13] L. Stadelmeier, D. Schneider, J. Zolner, and J. J. Gimenez, "Channel Bonding for ATSC 3.0," *IEEE Trans. Broadcast.*, vol. 62, no. 1, March 2016.
- [14] C. Regueiro *et al.*, "SHVC and LDM Techniques for HD/UHD TV Indoor Reception," in *2015 IEEE International Symposium on Broadband Multimedia Systems and Broadcasting (BMSB)*, June 2015, pp. 1–6.
- [15] *ATSC Standard - Physical Layer Protocol*, ATSC (Advanced Television Systems Committee) Std. A/322, Rev. 2017, February 2017.
- [16] S. M. Alamouti, "A Simple Transmit Diversity Technique for Wireless Communications," *IEEE Journal on Selected Areas in Commun.*, vol. 16, no. 8, pp. 1451–1458, Oct 1998.
- [17] D. Vargas, D. Gozalvez, D. Gomez-Barquero, and N. Cardona, "MIMO for DVB-NGH, the next generation mobile TV broadcasting," *IEEE Communications Magazine*, vol. 51, no. 7, pp. 130–137, July 2013.
- [18] T. Shitomi, E. Garro, K. Murayama, and D. Gomez-Barquero, "MIMO Scattered Pilot Performance and Optimization for ATSC 3.0," *IEEE Trans. Broadcast.*, vol. in press, 2018.
- [19] D. Tse and P. Viswanath, *Fundamentals of Wireless Communication*. New York, NY, USA: Cambridge University Press, 2005.



**Eduardo Garro** is a R&D engineer at Mobile Communications Group (MCG) of the Institute of Telecommunications and Multimedia Applications (iTEAM) at Universitat Politècnica de Valencia (UPV). He received a M.Sc. degree in Telecommunications engineering and a second M.Sc. degree in Communications and Development of Mobile Services from UPV, Spain in 2013 and 2014 respectively.

In 2012, he joined the iTEAM, working with Agencia Nacional del Espectro (ANE), the spectrum regulator of Colombia on the coexistence between DTT and 4G (LTE) technologies. He has also participated on the planning and optimization of DVB-T2 networks in Colombia. He has been also involved in the standardization of the new U.S. Digital Terrestrial Television (DTT) standard, ATSC 3.0.

He is currently pursuing his Ph.D. degree in terrestrial broadcasting and is involved in the 5G-Xcast (Broadcast & Multicast Communication Enablers for the Fifth-Generation of Wireless Systems) project. His research activities are focused on Non-Orthogonal Multiple Access (NOMA), multiple antenna systems (MIMO), and realistic channel estimation methods in broadcasting networks.



**Carlos Barjau** received his M.Sc degree in telecommunication engineering, Spain, in 2013. He is currently a Ph.D student at UPV, while working as a R&D engineer in Institute of Telecommunications and Multimedia Applications (iTEAM) since 2012. He has worked in Software implementations of diverse Broadcast standards, such as DVB-T2 and more recently, ATSC 3.0. He also has experience in broadcast solutions over 4G cellular networks such as eMBMS. His research interests involve efficient software implementations of receivers for broadcast

technologies, CUDA and OpenCL programming, novel demapping ideas for MIMO systems and architecture design for broadcast systems.



**David Gomez-Barquero** received the double M.Sc. degrees in telecommunications engineering from the Universitat Politècnica de Valencia (UPV), Spain, and the University of Gävle, Sweden, in 2004, the Ph.D. degree in telecommunications from the UPV in 2009; and he carried out a 2-year post-doc at the Fraunhofer Heinrich Hertz Institute, Germany.

He is a Senior Researcher (Ramon & Cajal Fellow) with the Institute of Telecommunications and Multimedia Applications, UPV, where he leads a research group working on next generation broadcasting technologies. He held visiting research appointments at Ericsson Eurolab, Germany, the Royal Institute of Technology, Sweden, the University of Turku, Finland, the Technical University of Braunschweig, Germany, the Sergio Arboleda University of Bogota, Colombia, the New Jersey Institute of Technology, USA, and the Electronics and Telecommunications Research Institute, South Korea.

Dr. Gomez-Barquero has been since 2008 actively participating in the digital television standardization, including DVB-T2, T2-Lite, DVB-NGH, and ATSC 3.0. He is an Associate Editor of the IEEE TRANSACTIONS ON BROADCASTING. He edited the book *Next Generation Mobile Broadcasting* (CRC Press, 2013); he is the coordinator of the 5G-PPP project 5G-Xcast (Broadcast & Multicast Communication Enablers for the Fifth-Generation of Wireless Systems).



**Jeongchang Kim** received the B.S. degree in electronics, communication and radio engineering from Hanyang University, Seoul, South Korea, in 2000 and the M.S. and Ph.D. degrees in electronic and electrical engineering from the Pohang University of Science and Technology (POSTECH), Pohang, South Korea, in 2002 and 2006, respectively. From 2006 to 2008, he was a Full-Time Researcher with POSTECH Information Research Laboratories, Pohang, and from 2008 to 2009, he was with the Educational Institute of Future Information Technology, POSTECH, as a Research Assistant Professor. From 2009 and 2010, he was with the Broadcasting System Research Department, Electronics and Telecommunications Research Institute as a Senior Researcher. In 2010, he joined the Division of Electronics and Electrical Information Engineering, Korea Maritime and Ocean University, Busan, South Korea, where he is currently a Full Professor. His research interests include MIMO, OFDM, DTV transmission, digital communications, and IoT platforms.



**Sung Ik Park** received the BSEE from Hanyang University, Seoul, Korea, in 2000 and MSEE from POSTECH, Pohang, Korea, in 2002, and Ph.D. degree from Chungnam National University, Daejeon, Korea, in 2011 respectively.

Since 2002, he has been with the Broadcasting System Research Group, Electronics and Telecommunication Research Institute (ETRI), where he is a senior member of research staff. His research interests are in the area of error correction codes and digital communications, in particular, signal

processing for digital television. In addition, he received a *Scott Helt* memorial award of IEEE TRANSACTIONS ON BROADCASTING in 2009, outstanding paper award of 2012 IEEE CONFERENCE ON CONSUMER ELECTRONICS (ICCE), and best paper award of 2012, 2014, 2015 IEEE SYMPOSIUM ON BROADBAND MULTIMEDIA SYSTEMS AND BROADCASTING (BMSB) respectively.

He currently serves as an associate editor of the IEEE TRANSACTIONS ON BROADCASTING and distinguished lecturer of IEEE BROADCASTING TECHNOLOGY SOCIETY.



**Namho Hur** (S'96-A'00-M'04) received the B.S., M.S., and Ph.D. degrees in electrical and electronic engineering from Pohang University of Science and Technology (POSTECH), Pohang, Korea, in 1992, 1994, and 2000. He is currently with the Broadcasting and Media Research Laboratory, Electronics and Telecommunications Research Institute (ETRI), Daejeon, Korea.

He was an Executive Director of Association of Realistic Media Industry (ARMI) in Korea. ARMI was established to promote realistic media industry including 3DTV and UHDTV broadcasting industry. Also he is an adjunct professor with the Department of Mobile Communications and Digital Broadcasting, University of Science and Technology (UST) in Korea since 2005 September. For the collaborative research in the area of multi-view video synthesis and the effect of object motion and disparity on visual comfort, he was with Communications Research Centre Canada (CRC) from 2003 to 2004.

His main research interests are in the field of next-generation digital broadcasting systems such as terrestrial UHD broadcasting system, UHD digital cable broadcasting system, mobile HD broadcasting system, and backward-compatible 3D-TV broadcasting systems for mobile, portable, fixed 3D audio-visual services.